JOURNAL OF SOLID STATE CHEMISTRY 76, 290–300 (1988)

Defect Fluorite-Related Superstructures in the Bi_2O_3–V_2O_5 System

WUZONG ZHOU

Department of Physical Chemistry, University of Cambridge, Lensfield Road, Cambridge CB2 1EP, United Kingdom

Received January 4, 1988; in revised form April 25, 1988

The ternary oxides in the compositional range from Bi_2O_3 to $BiVO_4$ have been investigated using electron diffraction and high-resolution electron microscopy. With small concentrations of vanadium, a solid solution based on γ-Bi_2O_3 was found to occur, but at greater vanadium contents, a $3 \times 3 \times 3$ superstructure derived from fluorite was first observed, followed by a family of triclinic superstructures containing fluorite-like and pyrochlore-like basic units. The details of these structures are discussed. © 1988 Academic Press, Inc.

Introduction

Using X-ray diffraction methods, several compounds and one solid solution range have been identified previously in the compositional range between Bi_2O_3 and $BiVO_4$. $(Bi_2O_3)_{0.975}(V_2O_5)_{0.025}$ was identified as a β-Bi_2O_3 (*1*) structure by Sekiya *et al.* in 1985 (*2*); $Bi_{25}VO_{40}$ is a Sillenite phase (γ-Bi_2O_3 (*3*)) reported by Kargin *et al.* in 1982 (*4*), in which V occupied 50% of the tetrahedral sites; and a compound $7Bi_2O_3$–V_2O_5 was found by Smolyaninov and Belyaev in 1963 (*5*), which apparently formed a continuous series of solid solutions with Bi_2O_3 over all compositions and with $BiVO_4$ at a minimum composition of 37.5 mole% V_2O_5, 870°C. No further information was given for the 7 : 1 composition and the solid solutions. In addition, Panchenko *et al.*, in 1983 (*6*), identified $Bi_{14}V_4O_{31}$ as a monoclinic compound with a = 1.9720, b = 1.1459, c = 8.0160 nm and β = 90.5°, but no structural details were given. Bush *et al.* (*7*), in 1985, identified $Bi_4V_2O_{11}$ as an orthorhombic compound with unit cell parameters of a = 1.684, b = 1.662, and c = 1.55 nm. This structure was deduced to be isotypical with Bi_2BO_5 (B = Ge, Si) and Bi_2BO_6 (B = W, Mo) in which sheets of V–O polyhedra are intergrown with layers of composition $Bi_2O_2^{2+}$.

In previous work performed in these laboratories (*8–11*), the systems Bi_2O_3–M_2O_5 (M = Nb, Ta) have been discussed. With a low M_2O_5 content (<5%), it was noted that the β-Bi_2O_3 structure could be quenched to room temperature, while in the $Bi_2O_3 : M_2O_5$ range of 9 : 1 to 3 : 1, the high-temperature phase of Bi_2O_3, namely, the δ-form (*12*), could be stabilized at room temperature. In this defect fluorite phase, M cations tended toward an ordered arrangement, consequently forming superstructures, in which the most Bi_2O_3-rich compositions were designated type I, where M cations were completely isolated from each other, occupying the body cen-

0022-4596/88 $3.00

tering positions in a 2 × 2 × 2 superlattice based on a fluorite subcell; with higher M_2O_5 content, a phase designated type II, in which MO_6 octahedra formed pyrochlore-like groups in an ordered arrangement on all (111) planes of a very large cubic unit cell, such as an 8 × 8 × 8 superunit cell with typical composition of 4 : 1, was observed. Through an intermediate type III phase, this being tetragonal at the 3 : 1 composition in the Bi_2O_3–Nb_2O_5 system but monoclinic at the 2 : 1 composition in the Bi_2O_3–Ta_2O_5 system, the fluorite-like sublattice then gives way to a perovskite one, as evidenced by monoclinic superstructures, designated type IV, based on $n = 1$ and $n = 2$ members of the Aurivillius series of phases. In these systems, the previously deduced model of extensive solid solution is not absolutely correct, as each could be divided into several solid solution ranges with, in each case, the cation ordering resulting in a characteristic type of structural arrangement.

In this present work, another ternary oxide system, namely Bi_2O_3–V_2O_5 is discussed. Following a γ-Bi_2O_3-like solid solution, type I- and type II-like phases, both based on the defect fluorite subcell, were determined by high-resolution electron microscopy and computer image simulations as a 3 × 3 × 3 cubic superstructure and a family of many triclinic compounds with large unit cells.

Experimental

The raw materials Bi_2O_3 and V_2O_5, of purity 99.9 and 99.6%, were used in the preparation of the ternary oxides. Weighed mixtures of the two components were ground with acetone for a few minutes in an agate mortar and pestle, dried in air, and then placed in a furnace heated at the desired temperature in a pure oxygen atmosphere, the specimen being quenched to room temperature directly upon completion of the preparation. The starting compositions, heating temperatures, and initial preparation times are listed in Table I. The main phases present were deduced by the analysis of X-ray and electron diffraction patterns.

TABLE I

LIST OF SPECIMEN PREPARATIONS

Starting composition (Bi_2O_3 : V_2O_5)	Heating temperature (°C)	Initial time (hr)	Main phase (type)
60 : 1	820	116	γ-form
45 : 1	820	116	γ-form
31 : 1	820	88	γ-form
25 : 1	830	187	γ-form
61 : 3	830	169	γ-form
19 : 1	820	162	γ + I
15 : 1	820	166	γ + I
25 : 2	820	98	γ + I
10 : 1	825	117	γ + I
9 : 1	825	96	I
8 : 1	825	117	I*
7 : 1	830	187	I*
6 : 1	820	190	II
4 : 1	820	190	II
7 : 2	800	168	II
2 : 1	800	136	Orthorhombic
1 : 1	620	195	Monoclinic

Initial characterization of the samples was by X-ray powder diffractometry (XPD). Compositional homogeneity was investigated using energy-dispersive X-ray microanalysis (EDS) within a Jeol-200CX electron microscope operating at 200 kV. Determination of supercell parameters was by selected area electron diffraction (SAED) and details of the structures were deduced from direct imaging using high-resolution electron microscopy (HREM) and computer image simulations. HREM images were recorded at a magnification of 500,000× over a range of objective lens focal increments, using a new type of side-entry specimen stage (C_s = 0.52 mm, C_c = 1.05 mm, with absolute information limit ca. 0.18 nm) (*13*) and computer-simulated

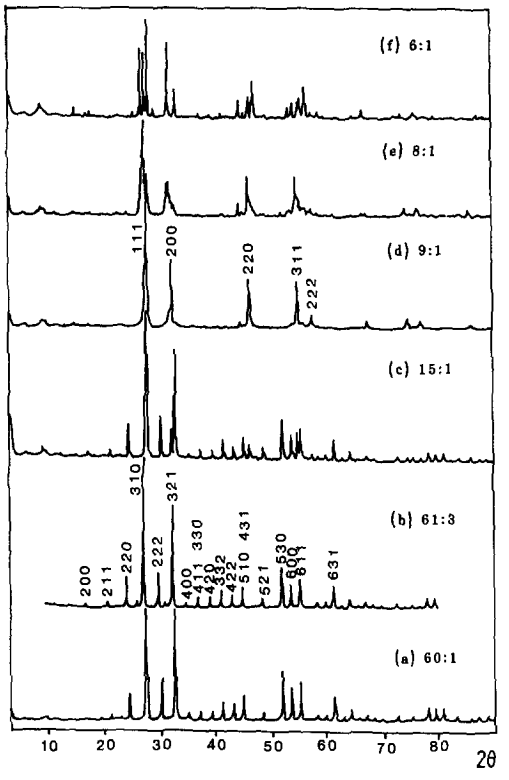

FIG. 1. X-ray powder diffraction patterns of some compositions in the Bi_2O_3–V_2O_5 system. The ratios of $Bi_2O_3 : V_2O_5$ are indicated. That of 61 : 3 is indexed onto the γ-Bi_2O_3-like unit cell and that of 9 : 1 onto a fluorite subunit cell.

model images were calculated according to the multislice method (*14, 15*) using programs especially developed for use with very large unit cells (*16*). Because of the strongly scattering nature of the specimens, the so-called Scherzer focus position was not necessarily the optimum one, and most images were recorded at considerably greater values of underfocus, where the resolution-limiting factor of beam divergence was reduced.

Results and Discussion

The XPD spectra indicated several different phases in the compositional range examined (Fig. 1). $Bi_2O_3 : V_2O_5$ ratios in the range 60 : 1 to 61 : 3 showed clearly a γ-Bi_2O_3-like structure with no detectable contaminant phases. From 19 : 1 to 10 : 1, another fluorite-like cubic phase coexisted with this γ-phase, the content of this new phase increasing as the proportion of V_2O_5 increased and at 9 : 1, this fluorite-like phase became the only one present. With further addition of V_2O_5, the cubic phase transformed gradually to a triclinic structure, the transformation being complete at 6 : 1. This latter structure was then retained until the composition reached 2 : 1 when an orthorhombic phase appeared (W. Zhou *et al.*, in preparation). From EDS, SAED, and HREM studies at each composition, further details of the structures could be elucidated.

γ-Bi_2O_3-like Structure (*Sillenite Phase*)

EDS results agreed with this structure type very well. Using the ratio of Bi $L\alpha$ and V $K\alpha$ emission lines and the reference material of freshly prepared $BiVO_4$, it was confirmed that the composition of this γ-Bi_2O_3-like structure could cover a range from 60 : 1 to 12 : 1, rather than constituting a single compound $Bi_{25}VO_{40}$. The unit cell of the γ-Bi_2O_3 structure is body-centered cubic with a = 1.02 nm (*3*). All cation and anion positions have been previously determined and there are only two tetrahedral sites. As given by the accepted general formula of this structure, $Bi_{24}[M^{m+}O_4][N^{n+}O_4]O_{32}$, with $m + n = 8$, only one V^{5+} cation could be introduced into the lattice, the limiting composition then being $Bi_{25}VO_{40}$ as previously reported. When the content of V was less than this, for example, $Bi_{25+x}V_{1-x}O_{40}$, xBi^{5+} cations were expected to occupy the remainder of the tetrahedral sites, which were normally occupied by V^{5+}, this being similar to the behavior found in pure γ-Bi_2O_3. Alternatively, Bi^{3+} could occupy the remainder of the tetrahedral sites, leaving some anion vacancies in

the lattice, as suggested by Aurivillius and Sillen in 1945 (*17*). In the present work, however, the ratio V : Bi could not only be less than 1 : 25 but also greater than this figure, the composition extending to $Bi_{25-x}V_{1+x}O_{40}$. In this case, xV^{5+} cations could be reduced from 5+ to 3+ and the composition would not extend beyond $Bi_{24}V_2O_{40}$ as confirmed by the EDS results discussed above.

The β-Bi_2O_3-like structure found by Sekiya *et al.* (*2*), has not been observed in the present work. Bearing in mind that Bi-rich specimens in the Bi_2O_3–Nb_2O_5 system can be produced in several modifications depending upon the preparation conditions (*18*), a similar phenomenon could be expected in this system. However, when quenched from 820°C to room temperature, only the γ-Bi_2O_3-like form was observed in Bi-rich compositions, probably because the smaller cation, V^{5+}, is more likely to form the γ-type structure which is considerably distorted from the fcc δ-form or the approximately cubic β-form.

Many SAED patterns and HREM images have been taken from different compositions in the γ-Bi_2O_3-like range, no significant differences being found among them. It was noted that, with the maximum amount of reduced V cations present, this phase was not produced without another phase being present, but always existed in equilibrium with an fcc phase (Fig. 1c). This will be discussed further below.

Type I Structure

The face-centered cubic phase observed with the γ-form in the 19 : 1 composition became the only phase in 9 : 1 and was designated type I.

On all the SAED patterns from composition 9 : 1, the observed diffraction maxima indicated a threefold repeat on a fluorite-like sublattice, with those corresponding to the fluorite cell being much stronger than the rest (Fig. 2). In this case, the simplest type I structure was therefore a $3 \times 3 \times 3$ superstructure derived from the fluorite lattice with possibly the same space group of $Fm3m$. Using the principle of the type I structure in the Bi_2O_3–Nb_2O_5 system (*18*) and ordering the guest cations appropriately in the lattice, a model for this $3 \times 3 \times 3$ superstructure has been built up with composition $Bi_{100}V_8O_{170}$. The cation arrangement of this model is shown in Fig. 3a. Four V atoms occupy the corners and face centers with another four V atoms in positions of (32*f*) 3*m*(1/3, 1/3, 1/3), (1/3, 5/6, 5/6), (5/6, 1/3, 5/6), and (5/6, 5/6, 1/3) of space group $Fm3m$. The calculated image from this model matches the real one quite well (Fig. 2c). It has, however, to be pointed out that this cation arrangement is not the only possibility for the type I structure, as V atoms occupying the other equivalent positions of (32*f*) 3*m* in the space group $Fm3m$ will produce a similar image to that shown in Fig. 2c. Nevertheless, it is quite certain that the arrangement of V atoms in the type I structure is such that they are separated by Bi atoms, creating the relatively low contrast variation in the image, and that they are also ordered, creating the $3 \times 3 \times 3$ superstructure. This structural principle is similar to that of the type I phase in the Bi_2O_3–Nb_2O_5 and Bi_2O_3–Ta_2O_5 systems.

V atoms usually have four coordination of O^{2-} which was confirmed by a laser Raman study (I. E. Wachs, unpublished work). In the fluorite lattice, there must therefore be four anion vacancies surrounding each V. If there are $(108 - x)$ Bi atoms and xV atoms in each real unit cell, then O atoms should number $162 + x$ and anion vacancies should be $54 - x$, and consequently when there are no anion vacancies in the fluorite lattice except those surrounding V atoms, the composition represents the upper-limit for the type I structure, and x is equal to 10.8. This upper-limit of the cation ratio of Bi : V is then 97.2 : 10.8 or

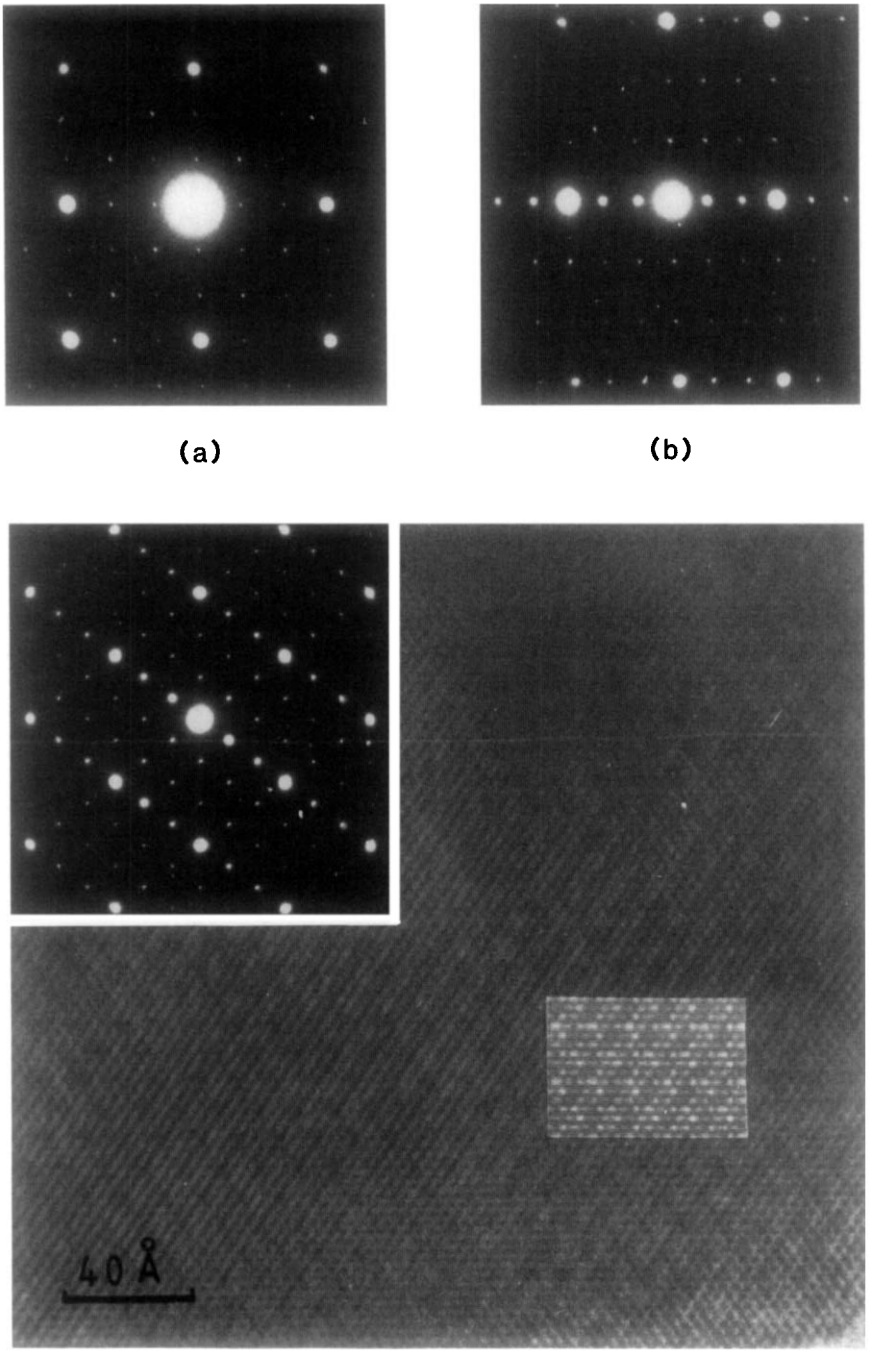

FIG. 2. (a and b) SAED patterns in the [001] and [112] projections and (c) HREM image and corresponding SAED pattern viewed down the (110) axis from $9Bi_2O_3$–V_2O_5. The inset of (c) is the calculated image from the model for the type I structure with the conditions: specimen thickness of 8 nm, lens defocus of 120 nm, and image resolution of 0.25 nm.

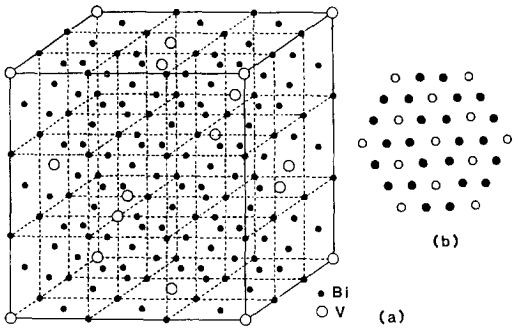

FIG. 3. (a) The cation arrangement in the model for the type I superstructure with the composition of $Bi_{100}V_8O_{170}$. (b) Cation arrangement on (111) plane in this model.

9 : 1, agreeing with the experimental stoichiometry very well. In this lattice, there are 108 cations. Consequently, the true composition could have a cation ratio Bi : V of 98 : 10 or 97 : 11. Considering that the compositional range of this type I structure extends from 14 : 1 to 9 : 1 as indicated by EDS, the typical composition $Bi_{100}V_8O_{170}$ for the model is reasonable, although two or three more Bi cations could still be substituted by V without change of structural type. This O^{2-} vacancy controlled composition limit supported the structural principle of the type I phase.

Because of the tetrahedral coordination of O^{2-} around V^{5+} cations, there is a tetrahedral arrangement of anion vacancies around V^{5+}, with three vacancies lying on one of the (111) planes of the cubic unit cell and all V cations lying on (111) planes, the ordering of these cations arising due to an interaction between anion vacancies. Consequently, the type I structure would be like the model shown and the cation arrangement on the (111) plane of the model is shown in Fig. 3b. It is interesting to compare the cation arrangement of this model with the type II model described in the next section and it is surprising that two such different arrangements on the (111) planes were relatively stable. When further V_2O_5 was added, no more Bi^{3+} in the (111) planes could be substituted and only those in between planes could be replaced, causing a reduction in the symmetry from cubic. Consequently, new triclinic phases then appeared.

Type II Structure

When the V_2O_5 content increased from 9 : 1 (Bi : V), it was impossible to retain the type I structure where all V cations were separated by at least one Bi cation. Consequently, V–O–V bonding was expected. In the compositions 8 : 1 and 7 : 1, a noncubic phase, designated type II (Fig. 1e), started to appear. The electron diffraction patterns were in agreement with the results of XPD, with many incommensurate diffraction maxima being observed in one of the ⟨111⟩ directions, and the relative intensities of the original maxima of the type I structure were altered, indicating that the structures of 8 : 1 and 7 : 1 compositions were intermediate phases between the type I and a new structure, type II (Figs. 4a and 4b). The latter represents a large family of many commensurate phases with the compositions from 6 : 1 to 4 : 1. It was noted that this phase transition was quite gradual and that EDS studies of any composition in this range indicated complete compositional homogeneity, suggesting that a clear phase boundary might not exist between type I and type II.

Many SAED patterns of the 6 : 1 composition have been indexed (Figs. 4c–4j). All of the prominent diffraction maxima correspond to a fluorite-like subcell and the weak maxima indicate a triclinic superstructure. Many series of SAED patterns have been taken while tilting the specimen grid in order to determine the true unit cell, and at least six triclinic phases were observed and their unit cells determined. However, in 6 : 1, the main phase was relatively simple, designated type IIa (Figs. 4c and 4d). The relationship between the fluorite sublattice and type IIa has been obtained as:

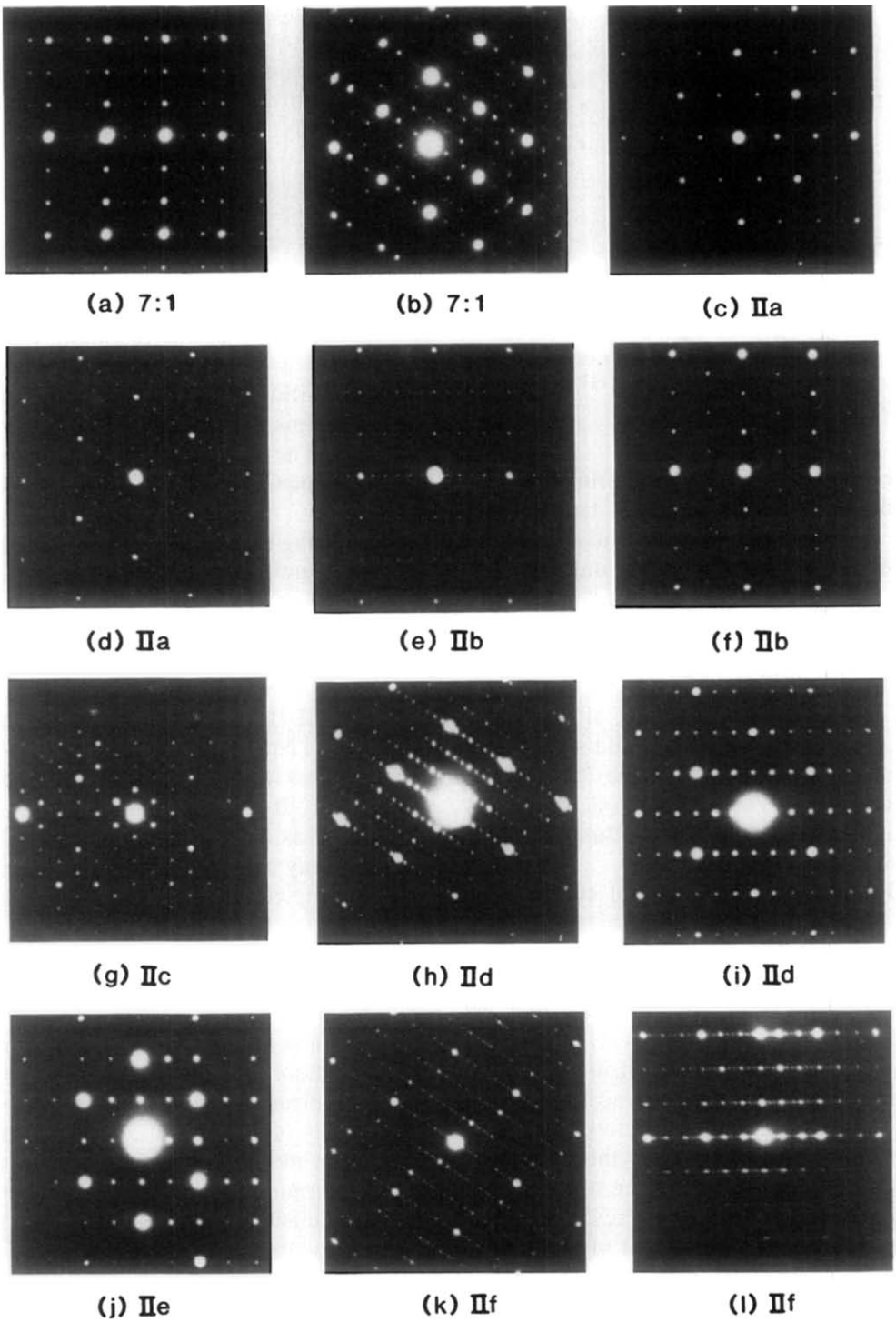

FIG. 4. (a and b) SAED patterns of $7Bi_2O_3$–V_2O_5 in the [112] and [110] projections and (c–l) SAED patterns of the type II family in the [110] (c, d, g–k) or [112] (e, f, l) projections of the fluorite subcell.

$$\mathbf{a}_{IIa} = 3/2\mathbf{a}_f + 3/2\mathbf{c}_f;$$
$$\mathbf{b}_{IIa} = 3/2\mathbf{b}_f + 3/2\mathbf{c}_f;$$
$$\mathbf{c}_{IIa} = -\mathbf{a}_f - \mathbf{b}_f + 4\mathbf{c}_f.$$

where **a, b, c** are unit cell vectors.

The real unit cell was then expected as $a_{IIa} = b_{IIa} = 1.17$, $c_{IIa} = 2.34$ nm, $\alpha = \beta = \gamma = 60°$, but a distortion of the lattice due to the loss of cubic symmetry exists and the real unit cell is actually $a_{IIa} = b_{IIa} = 1.17$, $c_{IIa} = 2.388$ nm, $\alpha = \beta = 57.77°$, and $\gamma = 60.0°$. This superstructure had 13.61 times the volume of the fluorite subcell. If the density was unchanged, in one complete unit cell, there are 54 cations including 7 or 8 V atoms.

When viewed down the ⟨110⟩ axis of the fluorite sublattice in the image (Fig. 6), the structure of type IIa $6Bi_2O_3$–V_2O_5 was clearly not cubic but based upon ordering on only one of the (111) planes of the fluorite subcell. If we suppose that in this type II structure, V cations form into tetrahedrally disposed units of four as in the Bi_2O_3–Nb_2O_5 system (*8*), a model could be built up as shown in Fig. 5a. Here the basic units containing V atoms resemble the pyrochlore-like units found in the Bi_2O_3–Nb_2O_5 system, except that they consist of four tetrahedra around V atoms, rather than octahedra as found previously. All V–O tetrahedral units lay on the main (111) plane of the fluorite subcell arranged in a diamond-like pattern and each such unit is linked to its neighbor by one Bi cation.

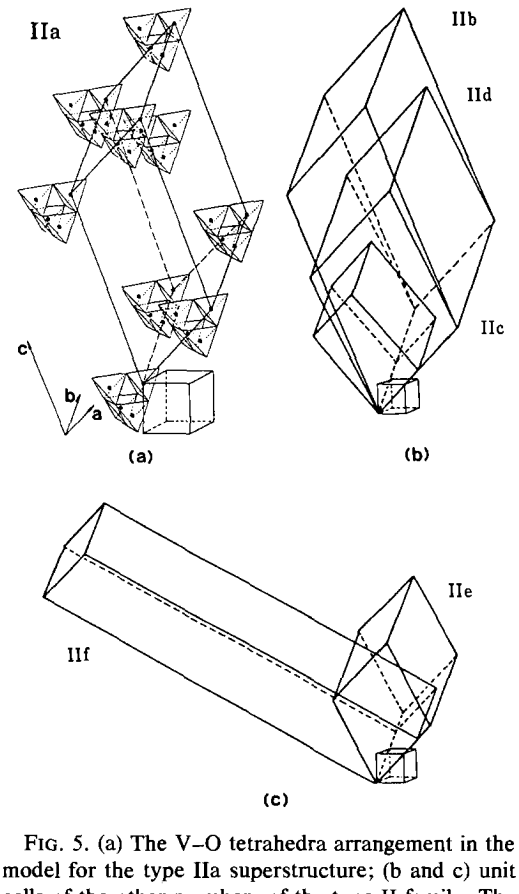

FIG. 5. (a) The V–O tetrahedra arrangement in the model for the type IIa superstructure; (b and c) unit cells of the other members of the type II family. The cubes show the fluorite subcell.

When this arrangement is compared with the model for the type I structure (Fig. 3), it is obvious that the type II structure is derived from the type I phase in a continuous transformation process as suggested above, when a point is reached where there are insufficient anion vacancies available to allow all V^{5+} cations to be completely isolated on (111) planes.

The calculated images from different thickness and objective lens defocus of this type II model match the experimental image quite well. Almost all the structural details on the image have been reproduced (Fig. 6).

As discussed above, the type II structure in this system occurs only with ordering of cations on one of the (111) planes and it is expected that the arrangement of V–O tetrahedra on such a (111) plane is even more stable than that in the type I structure, but the distance and relative positions of the V–O units between such planes is variable. Consequently, an infinite number of arrangements is possible, making the type IIa structure found here only one of a family of possible structures. In the compositional range 6:1 to 4:1, many members of this family have been observed.

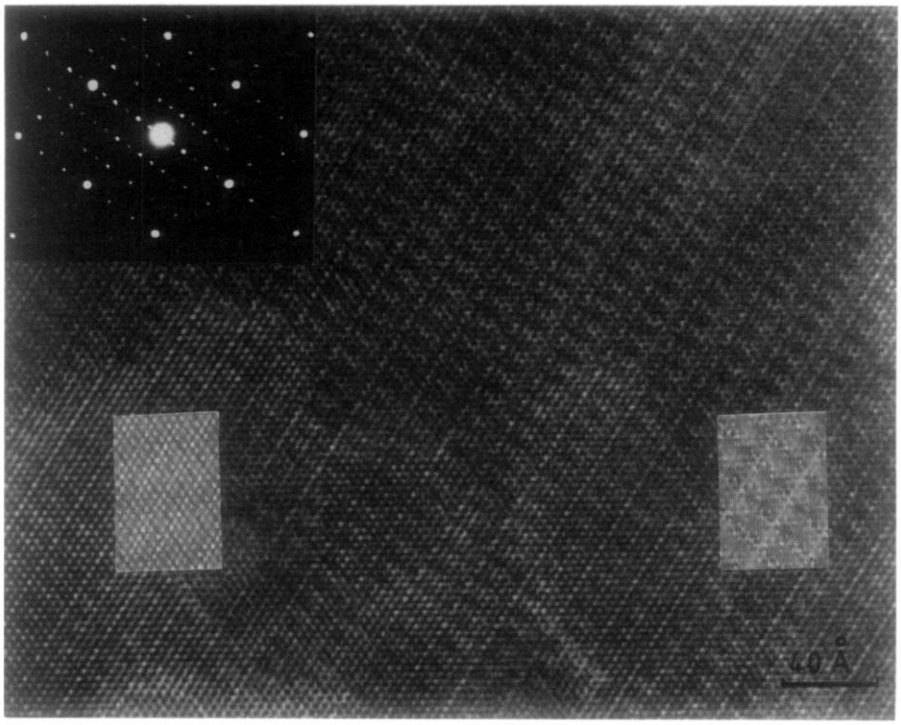

FIG. 6. HREM image of the type IIa structure in $6Bi_2O_3$–V_2O_5 viewed down the (110) axis of the fluorite subcell. The insets are the calculated images from the model for such structure with the conditions: specimen thickness of 2 and 4 nm (left and right), lens defocus of 95 and 105 nm, and image resolution of 0.25 nm.

Apart from the main phase discussed above, there were two other distinct members in the 6:1 composition. In Fig. 4, e and f could be indexed into a three dimensionally doubled unit cell of the type IIa, being designated as type IIb, and g could be indexed onto a very similar unit cell which derived from the fluorite sublattice by the relationship:

$$\mathbf{a}_{\mathrm{IIc}} = 3/2\mathbf{a}_{\mathrm{f}} + 3/2\mathbf{c}_{\mathrm{f}};$$
$$\mathbf{b}_{\mathrm{IIc}} = 3/2\mathbf{b}_{\mathrm{f}} + 3/2\mathbf{c}_{\mathrm{f}};$$
$$\mathbf{c}_{\mathrm{IIc}} = -3/2\mathbf{a}_{\mathrm{f}} - 3/2\mathbf{b}_{\mathrm{f}} + 3\mathbf{c}_{\mathrm{f}},$$

this being designated as type IIc. Another 6:1 sample was prepared using NaCl as a flux to promote the growth of larger crystals, and probably contained some Cl^- inside the structure which had not been removed by washing. The unit cell of this preparation was found to be larger than that of the pure 6:1 composition, an eightfold repeat in the main ⟨111⟩ direction of the fluorite-like subcell being observed. Figs. 4h and 4i showed that this structure was derived from the fluorite-like sublattice by the transformation:

$$\mathbf{a}_{\mathrm{IId}} = 3\mathbf{a}_{\mathrm{f}} + 3\mathbf{c}_{\mathrm{f}};$$
$$\mathbf{b}_{\mathrm{IId}} = 3\mathbf{b}_{\mathrm{f}} + 3\mathbf{c}_{\mathrm{f}};$$
$$\mathbf{c}_{\mathrm{IId}} = -3/2\mathbf{a}_{\mathrm{f}} - 3/2\mathbf{b}_{\mathrm{f}} + 5\mathbf{c}_{\mathrm{f}},$$

this being designated as type IId, and 4j was derived from the subcell by

$$\mathbf{a}_{\mathrm{IIe}} = 2\mathbf{a}_{\mathrm{f}} + 2\mathbf{c}_{\mathrm{f}};$$
$$\mathbf{b}_{\mathrm{IIe}} = 2\mathbf{b}_{\mathrm{f}} + 2\mathbf{c}_{\mathrm{f}};$$
$$\mathbf{c}_{\mathrm{IIe}} = -\mathbf{a}_{\mathrm{f}} - \mathbf{b}_{\mathrm{f}} + 3\mathbf{c}_{\mathrm{f}},$$

which was designated as type IIe.

When the composition approached 4 : 1 (Figs. 4k and 4l), the repeat indicated by the diffraction spots in the main ⟨111⟩ direction increased to 24-fold. All the SAED patterns could be indexed onto a unit cell derived from the subcell by the transformation:

$$\mathbf{a}_{\mathrm{IIf}} = 3/2\mathbf{a}_{\mathrm{f}} + 3/2\mathbf{c}_{\mathrm{f}}$$
$$\mathbf{b}_{\mathrm{IIf}} = 3/2\mathbf{b}_{\mathrm{f}} + 3/2\mathbf{c}_{\mathrm{f}};$$
$$\mathbf{c}_{\mathrm{IIf}} = -8\mathbf{a}_{\mathrm{f}} - 8\mathbf{b}_{\mathrm{f}} + 8\mathbf{c}_{\mathrm{f}},$$

this being designated as type IIf. These superunit cells, compared with the fluorite sublattice, are shown in Figs. 5b and 5c.

Many HREM images for these members of the type II family have been recorded and, except for their different unit cells, the details of the image contrast are similar to those of the type IIa. This indicated that the arrangement of cations on the main (111) plane is relatively stable, and the differences result from variations in the stacking of these units. Due to the tetrahedral coordination for V cations which was confirmed by the laser Raman study by I. E. Waches, it is impossible to form V_7O_x or larger units such as those found in the Bi_2O_3–Nb_2O_5 system (*8*). Even in the 4 : 1 or 7 : 2 compositions, the only way to accommodate the higher V_2O_5 content is to vary the arrangement of atoms in the main ⟨111⟩ direction in accordance with the reduced Bi^{3+} and anion vacancy contents. Therefore, the basic V–O unit in the type II structures in this system is the V_4O_{10} tetrahedron.

In all these structures, the two requirements of a nominal fourfold coordination for V and overall electrical neutrality must be met. If we suppose that all O^{2-} vacancies are around V cations, then for each V_4 tetrahedron, there are 13 O^{2-} vacancies. For the 4 : 1 composition, the minimum number of O^{2-} vacancies is 3.25 and the formula of this phase would be $Bi_4VO_{6.75}$, while electrical neutrality requires $Bi_4VO_{8.5}$. This implied that there were some extra O^{2-} which must fill the vacancies around V cations. This is possible, however, because the bond of V–O is shorter than that of Bi–O and V_4 tetrahedra can therefore leave additional space between V and Bi cations which allows some O^{2-} anions to occupy the vacancies. In this case, V cations might well have an approximate six coordination with four O atoms in close bonding and two O atoms substantially further away, as occurs with Mo in the bismuth molybdates. Then, for each V_4 tetrahedron, there are 5 anion vacancies. Each V cation has on average 1.25 O^{2-} vacancies, and if the composition is $Bi_{100-x}V_xO_{150-x}$, the number of O^{2-} vacancies is then $50 - x$. In the limiting composition, therefore, $x = 22.2$. The ratio of Bi : V is then 77.8 : 22.2 or 7 : 2. In practice, the 7 : 2 composition still retains the type II structure.

When further V_2O_5 was added into the oxide, the compound $Bi_4V_2O_{11}$ was produced. Although XPD spectrum indicated a similar unit cell to that reported by Panchenko *et al.* (*6*), SAED patterns and HREM images of $Bi_4V_2O_{11}$ showed very different image contrast than that expected from Bi_2BO_5 (*B* = Ge, Si) or the $n = 1$ Aurivillius phase Bi_2BO_6 (*B* = W, Mo). $Bi_2O_2^{2+}$ layers certainly did not exist in the structure, which seemed to be a similar phase to that of γ'-Bi_2MoO_6 (*19*). The full investigation of this structure is still in progress.

Conclusion

The γ-Bi_2O_3-type structure in the system Bi_2O_3–V_2O_5 is not only present as a compound of formula $Bi_{25}VO_{40}$ but can also exist as a solid solution in the compositional range Bi : V of 60 : 1 to 12 : 1. When this approaches its limiting value ($Bi_{24}V_2O_{40}$), it seems possible that some V^{5+} cations are reduced.

The previous results indicating that solid solutions exist between Bi_2O_3 and $7Bi_2O_3$–V_2O_5, and between the latter and $BiVO_4$,

determined from X-ray diffraction studies, have been shown here to be only a "first-order" approximation to the truth. The present study, using HREM, gives a "second-order" approximation, and indicates that the cation arrangement is far from random in these phases, but can be subdivided into two groups, namely, type I, where all V^{5+} cations are separated by at least one Bi^{3+} cation, and type II, where ordering of V^{5+} cations into distinct structural groups occurs. The behavior is exactly analogous to that found in the systems Bi_2O_3–Nb_2O_5 and Bi_2O_3–Ta_2O_5, and as is the case with these systems a clear distinction between the traditional definition of a solid solution or a series of distinct compounds cannot be made. Further work is in progress to investigate the possible occurrence of similar structural series in related systems.

Acknowledgments

I express my thanks to Fudan University in Shanghai for the financial support, to Dr. D. A. Jefferson for his encouragement and very helpful discussions, and to Professors J. M. Thomas and M. Alario-Franco for their assistance and advice on this work.

References

1. G. Gattow and D. Schutze, *Z. Anorg. Chem.* **328,** 44 (1964).
2. T. Sekiya, A. Tsuzuki, and Y. Torri, *Mater. Res. Bull.* **20,** 1383 (1985).
3. H. A. Harwig and J. W. Weenk, *Z. Anorg. Allg. Chem.* **444,** 167 (1978).
4. Yu. F. Kargin, A. A. Mar'in, and V. M. Skorikov, *Izv. Akad. Nauk. SSSR Neorg. Mater.* **18**(10), 1605 (1982).
5. N. P. Smolyaninov and I. N. Belyaev, *Russ. J. Inorg. Chem.* **8,** 632 (1963).
6. T. V. Panchenko, V. F. Katkov, V. Kh. Kostyuk, N. A. Truseeva, and A. V. Schmal'ko, *Ukr. Fiz. Zh. (Russ. Ed.)* **28**(7), 1091 (1983).
7. A. A. Bush, V. G. Koshelayeva, and Yu. N. Venevtsev, *in* Proceedings, Sixth Int. Meet. Ferroelec., *Jap. J. Appl. Phys.* **24**(Suppl. 24-2), 625 (1985).
8. W. Zhou, D. A. Jefferson, and J. M. Thomas, *Proc. R. Soc. London Ser. A* **406,** 173 (1986).
9. W. Zhou, D. A. Jefferson, M. Alario-Franco, and J. M. Thomas, *J. Phys. Chem.* **91,** 512 (1987).
10. W. Zhou, D. A. Jefferson, and J. M. Thomas, *J. Solid State Chem.* **70,** 129 (1987).
11. W. Zhou, D. A. Jefferson, and J. M. Thomas, submitted for publication.
12. H. A. Harwig, *Z. Anorg. Allg. Chem.* **444,** 151 (1978).
13. D. A. Jefferson, J. M. Thomas, G. R. Millward, K. Tsuno, A. Harriman, and R. D. Brydson, *Nature (London)* **323,** 428 (1986).
14. J. M. Cowley and A. F. Moodie, *Acta Crystallogr.* **16,** 609 (1957).
15. P. Goodman and A. F. Moodie, *Acta Crystallogr. Sect. A* **30,** 280 (1974).
16. D. A. Jefferson, G. R. Millward, and J. M. Thomas, *Acta. Crystallogr. Sect. A* **32,** 823 (1976).
17. B. Aurivillius and L. G. Sillen, *Nature (London)* **55,** 305 (1945).
18. W. Zhou, Ph.D. Thesis, University of Cambridge (1987).
19. D. J. Buttery, D. A. Jefferson, and J. M. Thomas, *Philos. Mag.* **53**(6), 897 (1986).